Using High Density EMG to Proportionally Control 3D Model of Human Hand

International Journal on Advanced Science Engineering Information Technology

Vol.13 (2023) No. 3
ISSN: 2088-5334

Using High Density EMG to Proportionally Control 3D Model of Human Hand

Firman Isma Serdana [a,*], Silvia Muceli [b,c], Dario Farina [c]

[a] *Electronics Engineering Department, PENS, Surabaya, Indonesia*
[b] *Electrical Engineering, Chalmers University of Technology, Gothenburg, Sweden*
[c] *Department of Bioengineering, Imperial College London, London, UK*
*Corresponding Author: *firmanisma@pens.ac.id*

***Abstract*— Control of human hand using surface electromyography (EMG) is already established in various mechanisms, but proportionally controlling magnitudes degrees of freedom (DOF) of humanoid hand model is still highly developed in recent years. This paper proposes another method to achieve a proportional estimation and control of human's hand multiple DOFs. Gestures in the form of American Sign Language (ABCDFIKLOW) were chosen as the targets, of which ten alphabetical gestures were specifically used following their clarity on its 3D model. Then the dataset of the movements gestures was simultaneously recorded using High-density electromyography (HD-EMG) and motion capture system. Sensor placements were on intrinsic - extrinsic muscles for HD-EMG and finger joints for the motion capture system. To derive the proportional control in time series between both datasets (HD-EMG and kinematics data), neural network (NN) and k-Nearest Neighbour were used. The models produced around 70-95 % (R index) accuracy for the eleven DOFs in four healthy subjects' hand. kNN's performance was better than NN, even if the input features were reduced either using manual selections or principal component analysis (PCA). The time series controls could also identify most sign language gestures (9 of 10), with difficulty was given on O gesture. The false interpretation was because of nearly identical muscle's EMG and kinematics data between O and C. This paper intends to extend its conference version [1] by adding more in-depth Results and Discussion along making other sections more comprehensive.**

***Keywords*— High-density electromyography; hand kinematics; neural network; k-nearest neighbor.**

Manuscript 27 Oct. 2022; revised 7 Dec. 2022; accepted 20 Jan. 2023. Date of publication 30 Jun. 2023.

I. INTRODUCTION

A variety of methods and techniques have been developed to control a robotic hand using an electromyography (EMG) signal. Starting with the simplest linear control, which can only reproduce 2-3 degrees of freedom (DOF) of hand movement (e.g. [2]), and progressing to more complex non-linear control, which can reproduce a high order of DOF in the finger and wrist (e.g. [3], [4]). Despite their abundance, currently commercialized control strategies are low in DOF (e.g., Ottobock Hands [5] and Open bionics [6]) and are not particularly capable of replicating human hand's complex movement, particularly in terms of digits control, limiting their functionalities.

Most research on the estimation of complex hand movements has utilized classification methods, which estimate gestures discreetly rather than proportionally [5], [6]. However, this approach is not sufficient for optimal use of advanced robotics, which require continuous and sequential control [7], [8]. Natural hand movements involve not only discreet movements but also continuous and simultaneous control of multiple degrees of freedom. Some researchers have attempted to estimate hand movements proportionally, but have focused mainly on forearm and wrist movements, limiting finger movement to grasping or closing [4].

According to the homunculus diagram [9], a significant portion of the brain (25%) is dedicated to controlling the hands and fingers. This shows the importance of hand movement in everyday human activities, such as manipulation of objects and communication through gestures, such as sign language. Therefore, the ability to control the digits is crucial for effectively performing complex gestures, such as sign language.

In recent years, the development of EMG-based hand exoskeletons has mostly been focused on grip and grasp gestures [10]. This is because attempts to control multiple

fingers through EMG are typically used for hand prosthetics. One study that attempted to estimate multiple finger movements was conducted by Smith *et al.* [11], but it only focused on the metacarpophalangeal joints of the hand and did not incorporate the other, more distal joints. Hioki *et al.* [12] proposed a method for estimating the angles of the proximal interphalangeal joints because of their higher range of motion compared to other finger joints. However, this study used only four channels and required multiple complex parameters for its configuration, resulting in compromises in accuracy.

In a study conducted by Ngeo *et al.* [13], multiple finger joints were estimated using a high computational regression model called Gaussian Process. This allowed for the prediction of all five fingers' joints, including more distal joints than previous studies. However, the study only estimated joint angles from basic flexion-extension gestures and required a larger computational time compared to using a neural network. The study had previously also controlled a finger exoskeleton for comparison with kinematics recording, but only for the index finger.

Chen *et al.* [14] conducted a study in 2019 that explored the potential use of motor unit discharge to determine the movement of five joints in hand. This was done using HD-EMG in the forearm to decode the discharge. However, the study was limited in that it only examined the correlation between the motor unit discharge and joint movement. Blana *et al.* [15] later conducted a study in the same year that proposed using an EMG-driven biomechanical model to control a hand prosthesis in a proportional manner. This model allowed for real-time control of the hand based on EMG signals, although it only estimated the movement of three joints in the thumb, index, and middle finger.

The purpose of Serdana [1] study is to propose a new approach to proportional hand control using high-density electromyography (HD-EMG). Previous research has demonstrated the potential of HD-EMG for controlling hand and finger movements [16]. In this study, we used HD-EMG to investigate whether simpler regression methods, such as neural networks and k-nearest neighbor, could be effective in controlling hand movements. We also examined the high-dimensional features of HD-EMG recordings to determine the optimal arrangement of surface electromyography. To reduce the complexity of future EMG recording experiments, we also used visual selection and principal component analysis to reduce the dimensionality of HD-EMG [3], [14].

In contrast to the common practice of only using extrinsic muscles for precise or proportional control of the hand [15], [17], we decided to include intrinsic muscles in our control scheme [18], [19]. Based on previous research on using intrinsic muscles for hand control, we believed that this would improve performance. We also studied whether using only intrinsic muscles for control would be sufficient for proportional control of the hand. Instead of using general bipolar surface EMG, which limited the finger exoskeleton's ability to grip/grasp, we used four-mm-spaced HD-EMG to provide a more detailed spatial representation of the small intrinsic muscle movements [20], [21].

In this study, we used high-density electromyography (HD-EMG) to estimate the kinematics of the fingers rather than their forces, unlike previous studies by Barsotti *et al.* [22]. The kinematics of the finger were recorded concurrently with the HD-EMG recording and were used for training and testing in proportional control, similar to the approach Ngeo et al. took[13]. However, our study focused on more complex gestures in the form of American Sign Language alphabets to examine the dexterity of human fingers in proportional control of hand exoskeletons. We employed neural network and k-nearest neighbor methods to map the HD-EMG features to the kinematics recordings. Our study presents a new proportional control method for estimating complex finger movements using multiple degrees of freedom and HD-EMG signals.

II. Material and Methods

A. Subject

In previous research, a new proportional control method for the hand was developed [13], [16]. In this study, healthy individuals with normal limbs were selected. Four male volunteers (aged 24±2.58) participated, all of whom were right-handed. Prior to the experiment, all subjects provided informed consent according to the ethical guidelines for research. Ethical approval was obtained for the study.

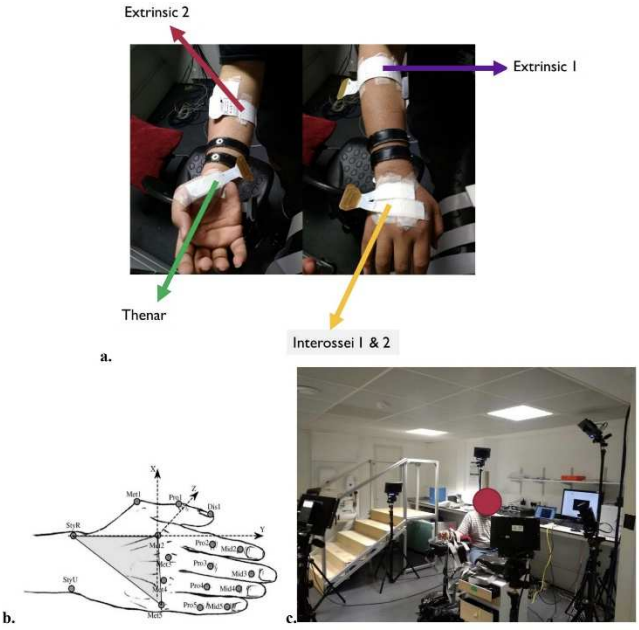

Fig. 1 a.) Placement of the HD-EMG grid, two 8 mm grids on the forearm (Extrinsic 1-2), and three 4 mm grids on the hand (Thenar, Interossei 1-2). b.) Marker placement for kinematics recording [25], StyR-U: the styloid process of ulnar and radius respectively, Met1-5: metacarpal, Pro1-5: proximal phalanges, Dist1: a distal phalanx of the thumb, and Mid2-5: middle phalanges of other fingers. c.) The position of the subject, surrounded by eight motion capture cameras focusing on the hand of the subject

B. Data Acquisition: HD-EMG

This study used two types of high-density electromyography (HD-EMG) grids to record muscle activity in the right arm. The 8 mm and 4 mm spaced grids were placed on the extrinsic and intrinsic muscles of the hand responsible for finger flexion and extension. The grids, produced by OT Bioelettronica, consisted of 13 columns and five rows. Two 8 mm spaced grids were placed around the circumference of the forearm, while three 4 mm spaced grids were placed on the intrinsic muscles of the hand. The subject's

skin was shaved and cleaned with alcohol prior to grid placement. This method was based on the suggestions of Muceli and Farina [16]. Electromyography (EMG) signals were collected using a monopolar configuration with 150 gain and a sampling rate of 2048 Hz. The signals were filtered with a bandpass filter set to a range of 10-500 Hz and digitally converted with 16 bits of precision. Two ground electrodes were placed on the wrist of the right arm. (Quattrocento, OT Bioelettronica, Torino, Italy) was the equipment used.

C. Data Acquisition: HD-EMG

Seventeen small infrared reflective markers were attached to the bones on the back of the hand (Figure 1b). Two markers were placed on the styloid process of the radius and ulnar bones, five markers on the heads of the metacarpal bones and proximal phalanges of each finger, four markers on the heads of the middle phalanges of the index to little finger, and one marker on the head of the distal phalange of the thumb. The markers were 8 mm in size and had a semi-hemispherical shape. No markers were placed on the distal head of the index to little fingers because the calculation of distal interphalangeal joints was not considered. The study utilized a motion capture system consisting of 8 infrared cameras (Smart-DX 6000, BTS Bioengineering, Quincy-USA) to capture markers on the subject. The data was then analyzed using the SmartTracker application. To minimize marker loss, 6 cameras were placed at the same height as the subject and 2 cameras were positioned at a higher position behind the subject (as shown in Figure 1c). This camera placement setup effectively ensured that at least 2-3 cameras were able to capture all markers. The sampling rate for recording kinematics was set to 250 Hz, and the calibration volume was adjusted to an extra small size (20 cm in all axes) along with the use of extra small markers (8 mm) to accurately capture the hand kinematics. This configuration was also utilized to prevent motion capture flickering and noise caused by marker switching and errors from closely spaced markers.

D. Experimental Procedures

The participants were asked to sit in a standard chair and position their elbow on a small table. They were allowed to adjust the height and rotation of the chair and table to ensure their comfort during the procedure. While in this position, they were instructed to maintain a static position with their hand, avoiding any movements except for finger movement. This was done to obtain clear recordings of finger muscle electromyography (EMG) and to prevent activation of muscles responsible for wrist movement. The distal side of the hand was required to be facing the front cameras, while the dorsal and palmar sides were visible to the side cameras. The hand was not allowed to supinate, pronate, or radially ulnar deviate during the recording (although in a resting state). This was done to prevent other muscles' activation and ensure the cameras captured all markers.

This study used American Sign Language (ASL) gestures for proportional tracking and recognition. The subjects were asked to perform ten alphabet gestures from a resting position. These gestures were selected for their variability and feasibility for motion capture [23], [24]. Prior to the experiment, the subjects were trained to avoid lag in their gestures. During the task, the subjects were given auditory cues to begin and end the gestures. The study involved recording the resting position of the subjects' fingers, as well as the position of their fingers when performing a specific gesture.

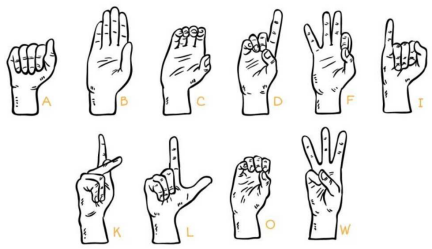

Fig. 2 10 alphabets of American Sign Language used for the experiments [26].

The study involved recording the resting position of the subjects' fingers, as well as the position of their fingers when performing a specific gesture. The resting position was recorded one second before and after the gesture was performed. During the gesture, the subjects were instructed to maintain the position for approximately four seconds without exerting excessive force. The gesture involved repeating ten alphabets in random order, and a total of 30 data points were collected from each subject. The subjects were allowed to take breaks during the recording process, but after 15 recordings, they were required to rest their hands to avoid fatigue. Both HD-EMG and kinematic data were recorded from the subjects' right arm simultaneously. Mirroring movements [16] was not used due to the potential for complications with the complexity of ASL gestures. An Arduino Uno was utilized to synchronize the Quattrocento and Smart DX 6000 systems using a rectangular signal triggered by the operator simultaneously with the auditory cues. The data was truncated synchronously with the stop auditory cue to eliminate unwanted recordings.

E. Data Post Processing: HD-EMG

In order to eliminate undesired noises such as motion artifacts, an offline bandpass filter (a 4th-order zero-lag Butterworth digital filter with a cut-off frequency of 20-400 Hz) was applied to the HD-EMG signals. After this, the EMG recordings were carefully examined to remove any channels with poor contact. The monopolar recordings were then transformed into bipolar channels aligned with the muscle fiber vector, reducing the number of channels from 320 to 267 and ensuring a common-mode rejection rate was applied to the recordings. The Fourier analysis of the post-processing showed that the HD-EMG data had an optimal frequency of less than 30 Hz. In order to only acquire muscle activity, a 16 Hz low pass filter (a 2nd order, zero lag, Butterworth digital filter) was also applied to the HD-EMG data [16].

The RMS features of the HD-EMG signals were extracted using a 15-millisecond window step, resulting in a low control rate of 60 Hz. RMS is commonly used in EMG feature extraction because it provides a reasonable estimate of EMG activity over a time window. Unlike previous studies [13], [16], the HD-EMG signals and their derivative features were not down-sampled to match the kinematics recording rate in order to avoid information loss [3].

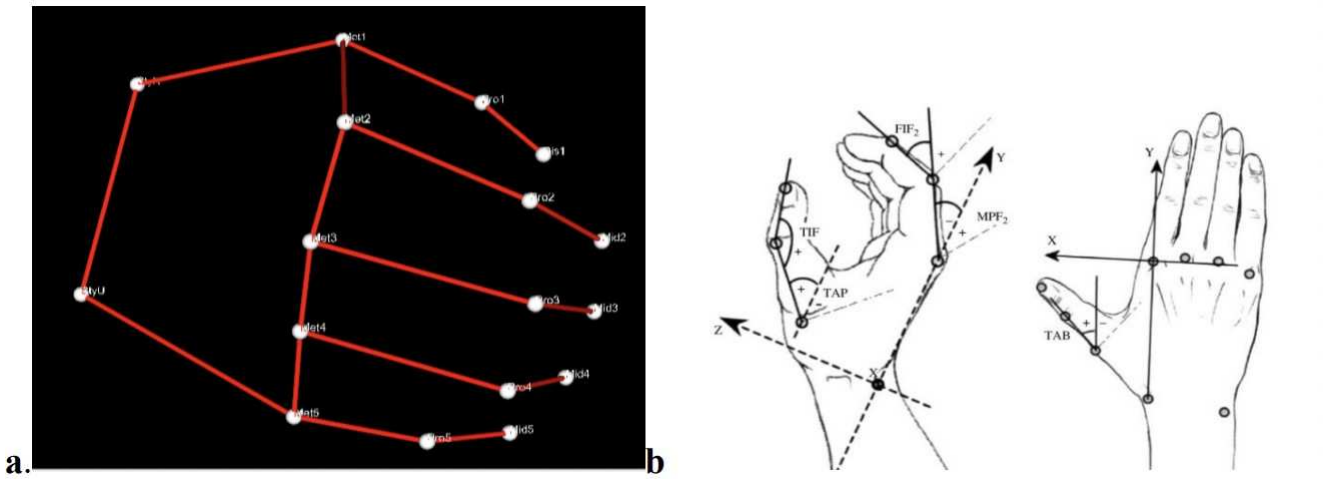

Fig. 3 a.) The model of the hand following Figure 1b with some links that interconnected each of the markers. This model can be the base for designing the soft exoskeleton. b.) Joint angle calculation based on Carpinella *et al.*[25], FIF = proximal interphalangeal joint flexion angle; MPF = metacarpophalangeal joint flexion angle; TIF = thumb interphalangeal joint flexion angle; TAP = thumb ante position angle; TAB = thumb abduction angle.

F. Data Post Processing: Kinematics Recording

The kinematics recording initially provided the position of markers in 2D space for each motion capture camera. Using Smart Tracker software, the 2D recording was then reconstructed into 3D space and a linked model was applied to the markers to create a visual representation of a real hand model. Eleven 1-dimensional angles were then calculated using Smart Analyzer software. The measurements did not include the distal interphalangeal joints of the index and little finger due to their low impact on hand gestures and their similar movement to the proximal interphalangeal joints [13]. Similarly, the abduction angles of the index and little fingers were also excluded from the calculations.

TABLE I
THE JOINT AND THEIR OWN THREE MARKERS USED TO CALCULATE THEIR ANGLES. 2-5 SPECIFY THE FINGER FROM THE RADIAL SIDE (INDEX, MIDDLE, RING AND LITTLE FINGER)

Joint	MarkersItalic
TIF	Met1-Pro1-Dis1
TAB	Pro1-Met1-Met2
TAP	Pro1-Met1-StyR
FIF2	Mid2-Pro2-Met2
FIF3	Mid3-Pro3-Met3
FIF4	Mid4-Pro4-Met4
FIF5	Mid5-Pro5-Met5
MPF2	Pro2-Met2-StyR
MPF3	Pro3-Met3-StyR
MPF4	Pro4-Met4-StyU
MPF5	Pro5-Met5-StyU

The angle data of the joints was then increased in its sampling rate to match the HD-EMG data (2048 Hz). As previously mentioned, some markers may be lost during the recording process of kinematics. Therefore, an interpolation or extrapolation was applied to compensate for this loss. Additionally, the noisy kinematics data caused by vibrating markers was smoothed using a moving average Gaussian filter, which functioned as a low-pass filter with a cut-off frequency of 1 Hz. Compared to other techniques, this filter was selected for its ability to produce output resembling a natural hand movement.

G. Feature Analysis

The use of high-density electromyography (HD-EMG) allows for the capture of a high number of features due to the small spacing between its channels. However, this also leads to a high degree of correlation between adjacent channels, resulting in redundant information within the dataset. This redundancy can be reduced through the use of visual selection and principal component analysis.

In this research, the visual selection was determined by the direction of the muscle's vector. For Extrinsic 1-2 and Interossei 1-2, a horizontal linear array of 14 bipolar channels and seven equally spaced channels were chosen. For the Thenar grid, a vertical linear array of five channels and three equally spaced channels were selected [16].

A principal component analysis was conducted on each grid's root mean square (RMS) features[16]. The first principal components were able to explain 70% of the variance in the RMS features for all subjects. Therefore, we examined the potential use of the first 14-7-1 components as input for training a regression model. (See Section 3.A for further details.)

In a previous section, we examined whether the use of extrinsic and intrinsic hand muscles resulted in different outcomes. The features were divided into two groups based on the recorded muscle type. The Extrinsic 1-2 grids were considered extrinsic features, while the Interossei 1-2 and Thenar grids were considered intrinsic features.

In order to compare the performance of the various feature configurations, a 3-way Analysis of Variance (ANOVA) was conducted with three main factors: subject, regression method, and input features. A post hoc Tukey-Kramer test was also used to determine significant differences among the groups within each factor. In addition, focused ANOVAs were performed to isolate and examine the specific differences between individual factors.

An investigation was conducted to determine if reducing the number of degrees of freedom in a hand model was possible. Although the results of the analysis were not implemented in this study, which focused on estimating multiple degrees of freedom simultaneously, it could

potentially be used as a method for recognizing American Sign Language gestures.

H. Joint Angle Estimation

In previous research, it has been demonstrated that electromyography (EMG) activity is closely related to muscle force [22], but some studies have also shown that it can be used to estimate joint angles [16]. In this study, we utilized neural network and k-nearest neighbor algorithms for training a regression model that predicts joint angles based on high-density EMG data.

This study utilized a convolutional neural network (NN) with two hidden Rectified Linear Unit (ReLU) layers. This type of NN was selected due to its demonstrated success in predicting complex bio-signals while maintaining low computational demands [26]. The two hidden layers had 100 and 50 neurons, respectively, which were determined to be the optimal hyperparameters. The input layer's neuron count depended on the number of input features used, and the output layer had a single output, resulting in 11 separate NNs trained for each angle. Using a single NN to estimate all angles yielded mediocre performance. However, for fairness in comparison, the hyperparameters of the NNs were not specifically modified for each angle. The dataset was divided into three parts for cross-validation during NN training, with 2/3 of the data used as the training/validation dataset (70/30% split) and the remaining part serving as an unseen dataset for testing the NN's performance.

K-Nearest Neighbour (kNN) is commonly utilized for classification purposes, but it can also be applied to regression or estimation tasks [27], particularly when working with a large dataset as input. This study utilized the kNN model with the same input and output characteristics as the previously discussed neural network. The hyperparameter k was set to 5 for all angle estimation comparisons to ensure fairness.

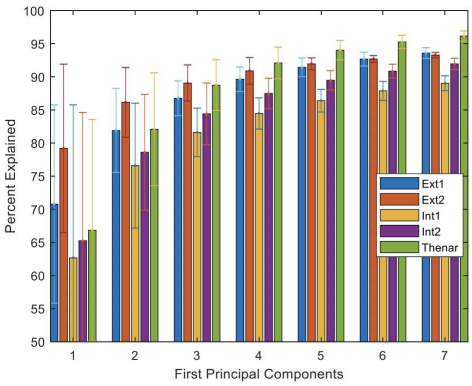

Fig. 4 The percentage of explained variance in each of the grids for seven first principal components. The Ext1-2 are Extrinsic grids, Int1-2 are Interossei grids, and Thenar is the thumb grid.

In order to make the output of the regression resemble natural movement, the same post-processing techniques used for kinematics recording were applied. This included smoothing with a Gaussian method and filtering with a low-pass Butterworth digital filter [13], [16]. The accuracy of the joint angle estimations was evaluated using Pearson's Correlation Coefficient and root mean square error. These metrics allowed for the determination of the variability and residual error between predicted and actual values [13].

III. Results and Discussion

A. Data Analysis

In this study, the high dimensionality of high-density electromyography (HD-EMG) was found to provide redundant information due to the large number of electrodes/channels. However, during the development phase, this feature can be useful in identifying the optimal EMG configuration for future use. Therefore, principal component analysis (PCA) was employed to analyze the potential optimal EMG configuration using HD-EMG grids. The first principal component overall accounted for 70% of the data, with varying percentages for different groups (70.78 ± 14.98 for Ext1, 79.18 ± 12.72 for Ext2, 62.67 ± 23.098 for Int1, 65.24 ± 19.36 for Int2, and 66.81 ± 16.73 for Thenar) (Figure 4).

The first 7 principal components were found to explain 90% of the data [16], constituting a good explanation of the entire dataset. Therefore, these 7 components were used to train the regression model. For a more detailed explanation of the data, the first 14 principal components were also used, explaining 95% of the data. A repeatability test of finger angles showed that the kinematics recordings were all repeatable for each alphabet in all four subjects [25]. In this study, the first seven principal components were found to adequately explain 90% of the data, and these components were used to train a regression model. To provide a more comprehensive explanation of the data, the first 14 principal components were also utilized, which explained 95% of the data. The repeatability of the kinematic recordings was confirmed (p>0.05) through an analysis of variance, indicating that the recordings were consistent across subjects for all alphabets tested (Carpinella *et al.* 2006 [25]).

While each individual subject had multiple p-values above 0.05, this did not occur consistently across all angles and letters. As previously noted by Weiss and Flanders [23], the high degrees of freedom in the hand may be further reduced by using several degrees of freedom. Four principal components of the kinematics data were able to explain 90% of the data, as shown in Figure 5a.

In this study, we did not reduce the dimension of kinematic data in the regression phase as we focused on simultaneously controlling multiple degrees of freedom of the hand. However, it is still possible to design proportional control by reducing the kinematics dimension through the use of principal component analysis (PCA) [28]. Our findings show that the PCA provides information about the kinematics dataset's variability and that the different alphabets' PCs have distinct variability for each subject. The distribution of the first two PCs in Figure 5b demonstrates that the alphabets used did not overlap, not even in their standard deviation. The closest alphabets were only D and K, and O and C (as they are identical, as shown in Figure 2).

B. Overall Results

After conducting regression analysis, the simultaneous estimation of all eleven joint angles was performed using both neural network (NN) and k-nearest neighbor (kNN) regressors. The regressors were trained using 66% of the dataset and then tested on the remaining third. In general, both regressors were able to accurately follow the target joint angles, although there were some instances of significant

deviation. In the best cases, the R-value for the metacarpophalangeal and proximal interphalangeal joints reached 95% and 90%, respectively. However, the abduction of the thumb had poor performance compared to the other joints. In terms of root mean squared error (RMSE), the overall residual error was approximately 10%, with the lowest possible error being 5%.

In order to compare the various parameters modified in the regression process, Figure 7 can be utilized. The RMSE metric did not provide a clear significant difference between the input feature configurations, although the estimation accuracy was clearer in R. The best configuration was found to be using full grids as the input feature, as previously reported by Muceli and Farina [16], with kNN as the regression method (Overall R= 78.09 ± 5.49 % and RMSE= 12.21 ± 5.09 %). Using PCA1 in NN resulted in the most inferior performance, although it was faster (Overall R= 65.03 ± 2.66 % and RMSE= 11.67 ± 4.64 %). When ranking the performance, although not significantly different in most cases, PCA14 performed better than PCA7, and Sel14 performed better than Sel7.

In the analysis comparing the performance of NN and kNN regression models using PCA14 and Sel14 input features, no significant differences were found between the two configurations regarding R and RMSE values, except for the TAB angle. However, significant differences were observed between PCA7 and Sel7 in some angles in the NN model. In addition, the full grids feature in the NN model showed significantly different results compared to both reduced features in most angles, using both PCA and selection methods. There were no significant differences between NN and kNN when using full grids as input features. Furthermore, a post hoc Tukey-Krame's test revealed that kNN performed better than NN in most cases, with an overall improvement of approximately 4% ($p<<0.001$).

The results of the study showed that the use of extrinsic-only grids performed poorly compared to the full grids and even intrinsic grids only (R= 60% and RMSE= 20%). There were also significant differences between extrinsic-only and full-grid configurations in most angles with $p<0.05$. Interestingly, the intrinsic grids feature had no significant difference in most angles compared with the full grids feature ($R\geq 70\%$ and $RMSE\leq 11\%$). By using the first two principal components of the kinematic recording and prediction, the regression results could be classified into different gestures (which were not fully explored in this paper). As seen in Figure 5b, most distinct alphabet predictions (9 of 10 ASL gestures) provided a more unambiguous classification as they fell into the areas of real alphabet measurements (or closer to the real alphabet). However, identical alphabet (O-C) prediction results could be falsely interpreted. The O predictions were only in the areas of actual C, potentially resulting in false-positive results of O predictions as C.

This study developed a new method to simultaneously estimate eleven joint angles of the hand using high-density surface EMG. This method performed similarly to previous studies [13]–[15], despite using more complex gestures for estimation. The use of a simple Neural Network and k-Nearest Neighbour algorithms allowed for faster and lighter computation than the Gaussian Process proposed by Ngeo *et al*. [13].Despite using time-domain features (RMS), the inclusion of intrinsic hand muscles in this study resulted in equivalent performance to the method proposed by Chen *et al*. [14].

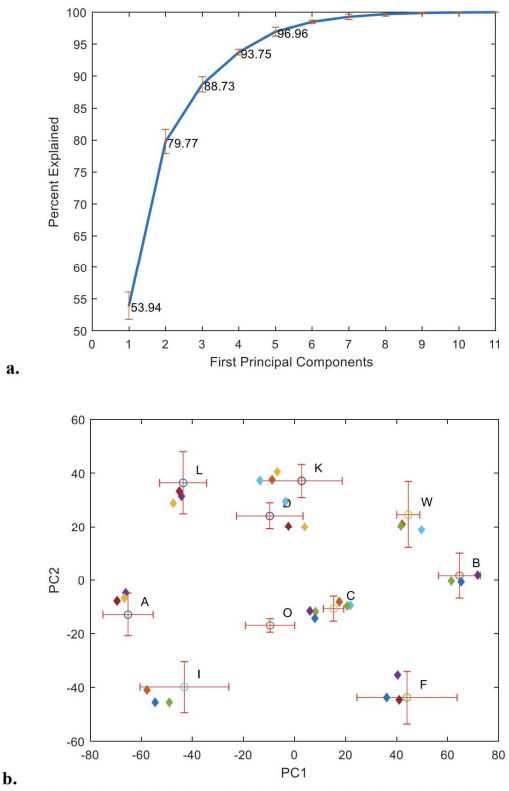

Fig. 5 a.) Percentage of kinematics data explained by its PCs. 2 PCs already explained 80 % of the data, although in[23], using all ASL alphabets, 4 PCs were needed to explain >80% of the data. b.) The scatter plot for the average of 2 first PCs in the kinematics dataset of all subjects. Each unfilled dot represents the ASL alphabets used in the experiment, along with their standard deviations. The diamond-shaped markers were the two first PCs of the predicted joint angles in Subject 3 using kNN with average RMSE = 10.78 ± 4.64 % and R = 80.65 ± 6.92 % in all DOFs.

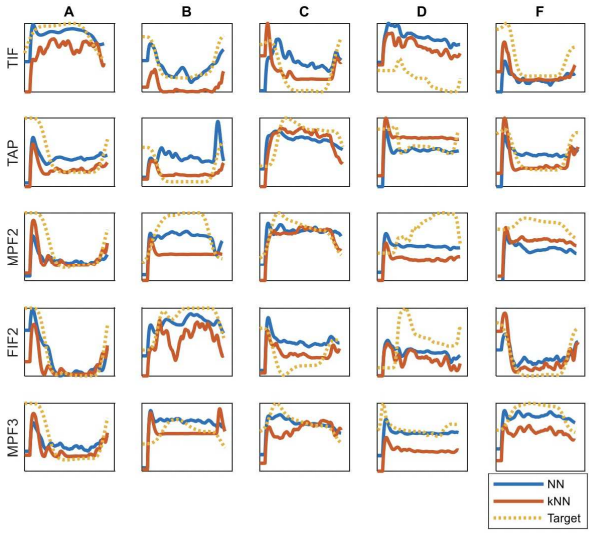

Fig. 6 An example of joint angle estimation between Neural Network (NN), k-Nearest Neighbour (kNN) and its actual output. Only A B C D F gestures, TIF, TAP, MPF2, FIF2 and MPF3 joint angles were shown for clarity. The dataset used was from Subject 3 using all bipolar channels as input. The overall performance for NN was R = 72.67 +/- 4.55 %, RMSE = 10.08 +/- 0.25 %; and for kNN was R = 80.4 +/- 0.82 %, RMSE = 11.37 +/- 0.83 %.

C. Feature Dimensions

The use of 14 channels along the length of the HD-EMG grids was shown to provide a reasonable estimation of joint angles, comparable to the use of the full grid. The use of seven channels also estimated joint angles well, with a correlation of 70% and an RMSE of 11%. However, using principal component analysis (PCA) delivered a slightly better estimation, as the values in PCA were projected values of all dimensions, unlike the visually selected features. Although the first principal component explained 70% of the data, the resulting estimation using this feature did not perform as well, with a correlation of 65% and an RMSE of 19%. Previous research [16] has also found that the more channels used, the better the performance of regression. The full grid performed significantly better than the reduced-channel configuration in a previous study.

In the real world, the use of a large array of bipolar electrodes placed perpendicular to the direction of muscle fibers was effective in controlling a hand exoskeleton. This is because the muscles in the hand are arranged radially [29]. Most commercial myo-control products also utilize this perpendicular electrode placement. The inclusion of intrinsic muscles in the configuration resulted in improved performance compared to using only extrinsic muscles, with an overall improvement of 10%. This is due to the fact that the extrinsic muscles include additional muscles that actuate the wrist, which will alter the EMG recording [30]. As shown in section 3.B and Figure 7c, both regressors (NN and kNN) paired with just intrinsic muscles as input characteristics performed similarly to the complete grids arrangement and much better than the extrinsic alone configuration. This indicates we can only anticipate finger kinematics using intrinsic muscles [31]. The size of the output feature (many DOFs of the hand) may also be lowered because most hand posture/gesture may be described by its various components [23].

The study found that using two principal components of hand kinematics was sufficient to explain 80% of the data variance. This reduction in the number of components could also improve the practical aspect of regression in terms of alphabet recognition, as shown in Figure 5b. However, the distribution of the first two PCs in Figure 5b can lead to a false positive recognition of the letter O as a letter C, as the differences between the two letters are difficult to distinguish in terms of joint angles and muscle activity (as shown in Figure 2). Using the distribution of the first three PCs was found to be more challenging in terms of alphabet recognition, as the predicted kinematics did not fall within the target alphabet areas.

D. Regression Methods

The k-Nearest Neighbour method performed similarly to the commonly used Neural Network in a regression analysis. However, when the input features were reduced, kNN showed better performance than NN. This difference in performance can be attributed to the techniques used in each regressor. The NN is a data-driven method that requires more data for accurate predictions, whereas the kNN is a pattern-driven method that can recognize patterns with any input features [27].

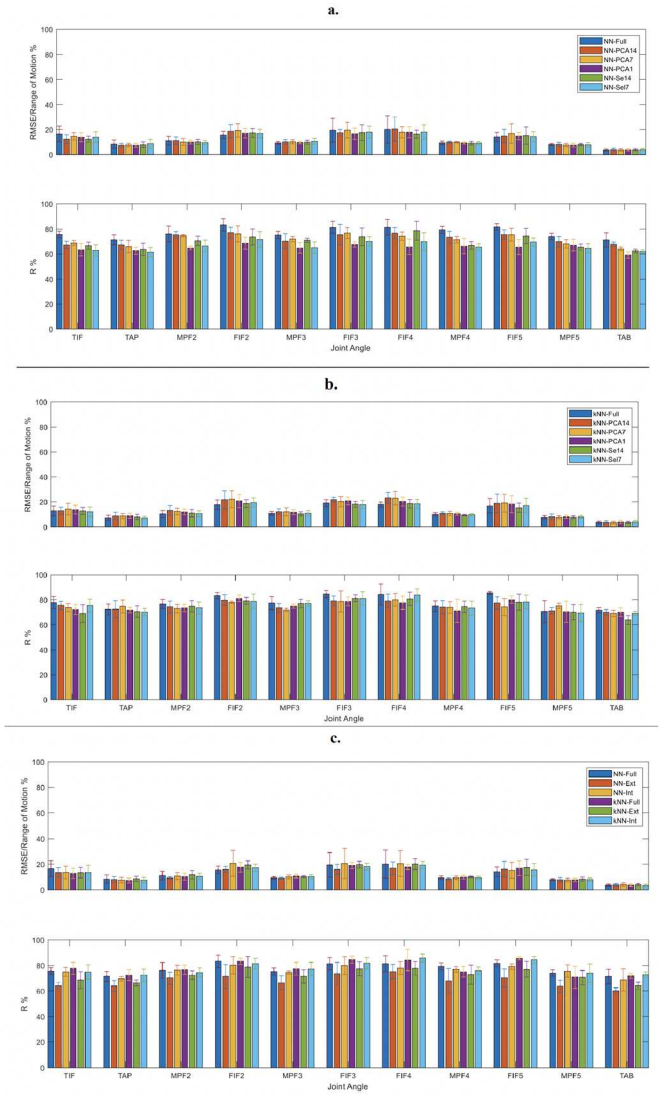

Fig. 7 RMSE and R-value in **a.)** NN and **b.)** kNN with different input features size. **c.)** RMSE and R-value in both NN and kNN, along with the use of only extrinsic/intrinsic muscles. The x-axis represents the joint angles, Full: using all bipolar channels, PCA14-7-1: using 14,7,1 first principal components, Sel14-7: using 14,7 selected channels, Ext: using only extrinsic grids, and Int: using only intrinsic grids.

In comparison to the Gaussian Process model proposed by Ngeo *et al.* [13], the k-nearest neighbor algorithm (kNN) demonstrated faster processing speeds with similar or comparable performance. Additionally, the kNN was able to predict a greater number of hand degrees of freedom compared to the biomechanical model of Blana *et al.* [15], with similar processing time. In practical application, the kNN also showed significantly faster performance than neural networks, depending on the machine used. This increased efficiency could be beneficial in implementing real-time proportional control of hand exoskeleton technology, as lower computational time can reduce the lag between user muscle activity and exoskeleton actuation.

E. Future and Implementations

In this study, the process of estimating joint angles was conducted offline, but the proposed method could also be applied in an online setting. It is worth noting that the high dimensionality of the HD-EMG data, using only the RMS feature, allows for the use of simple regression methods (NN and kNN) which reduces processing time compared to more

complex features and regressors used in other studies. This means that the delay in practical application will be minimal (around 100 ms) for real-time proportional control, although improved computational power in practical devices could enhance the processing time of more advanced methods. In future research, it may be worthwhile to explore the use of a real or virtual exoskeleton hand to evaluate the practicality of the proposed method. The subjects in this study were limited to a small number of healthy individuals with normal body composition.

In future research, it would be beneficial to include a larger sample size and a wider range of participants, including those who are not healthy, to strengthen the study results. The current experiment was limited to a static arm and wrist position in order to eliminate the influence of wrist motion. However, this issue can potentially be addressed by incorporating intrinsic muscle activity as a feature in the analysis. In order to apply this approach in clinical settings, a simpler setup for measuring hand kinematics, such as using IMU sensors for each finger, could be utilized [32]. Both HD-EMG and hand kinematics provide redundant information on muscular-postural activities. Applying the postural and muscular synergy analysis could help reduce this redundancy and improve cost-effectiveness, though this may be specific to the task at hand if the muscle-posture activities in the study are not varied enough.

IV. Conclusion

This study proposes a method for simultaneously estimating the eleven degrees of freedom of American Sign Language gestures using high-density electromyography (HD-EMG) data from extrinsic and intrinsic hand muscles. The reduction of HD-EMG data did not impact the system's performance, and the intrinsic muscles were found to be more effective than extrinsic muscles for estimating hand kinematics. The k-nearest neighbor regressor outperformed the neural network, particularly when using reduced input features. Our proposed approach has potential applications in the development of exoskeleton systems for hand kinematics estimation.

Acknowledgment

The authors thank Professor Dario Farina and Dr Silvia Muceli for the insight and general support to the study and Dr Alessandro Del Vecchio for discussion of the project plan.

References

[1] F. I. Serdana, "Controlling 3D Model of Human Hand Exploiting Synergistic Activation of The Upper Limb Muscles," *IES 2022 - 2022 International Electronics Symposium: Energy Development for Climate Change Solution and Clean Energy Transition, Proceeding*, pp. 142–149, 2022, doi: 10.1109/IES55876.2022.9888488.

[2] A. Theuer *et al.*, "Case Report: Optimizing Daily Function for People with Below-elbow Limb Deficiency with the SoftHand Pro.," *Open Journal of Occupational Therapy*, vol. 8, no. 4, pp. 1–9, Sep. 2020, doi: 10.15453/2168-6408.1602.

[3] M. H. Hasbani, D. Y. Barsakcioglu, M. K. Jung, and D. Farina, "Simultaneous and proportional control of wrist and hand degrees of freedom with kinematic prediction models from high-density EMG," *Proceedings of the Annual International Conference of the IEEE Engineering in Medicine and Biology Society, EMBS*, vol. 2022-July, pp. 764–767, 2022, doi: 10.1109/EMBC48229.2022.9871346.

[4] M. Nowak, I. Vujaklija, A. Sturma, C. Castellini, and D. Farina, "Simultaneous and Proportional Real-Time Myocontrol of up to Three Degrees of Freedom of the Wrist and Hand," *IEEE Trans Biomed Eng*, 2022, doi: 10.1109/TBME.2022.3194104.

[5] Ottobock, "bebionic Hand EQD | The most lifelike prosthetic hand." https://www.ottobock.com/en-us/product/8E70 (accessed Dec. 09, 2022).

[6] Open Bionics, "Open Bionics - Turning Disabilities into Superpowers." https://openbionics.com/en/ (accessed Dec. 09, 2022).

[7] M. N. Castro and S. Dosen, "Continuous Semi-autonomous Prosthesis Control Using a Depth Sensor on the Hand," *Front Neurorobot*, vol. 16, p. 51, Mar. 2022, doi: 10.3389/FNBOT.2022.814973/BIBTEX.

[8] P. Weiner, J. Starke, S. Rader, F. Hundhausen, and T. Asfour, "Designing Prosthetic Hands With Embodied Intelligence: The KIT Prosthetic Hands," *Front Neurorobot*, vol. 16, p. 25, Mar. 2022, doi: 10.3389/FNBOT.2022.815716/BIBTEX.

[9] R. F. Becker, "The cerebral cortex of man. By Wilder Penfield and Theodore Rasmussen. The Macmillan Company, New York, N.Y. 1950. 248 pp," *Am. J. Phys. Anthropol.*, vol. 11, no. 3, pp. 441–444, 1953.

[10] B. Xu *et al.*, "Natural grasping movement recognition and force estimation using electromyography," *Front Neurosci*, vol. 16, p. 1020086, Oct. 2022, doi: 10.3389/FNINS.2022.1020086.

[11] R. J. Smith, F. Tenore, D. Huberdeau, R. Etienne-cummings, and N. v Thakor, "Continuous Decoding of Finger Position from Surface EMG Signals for the Control of Powered Prostheses," *Crit. Rev., pp*, pp. 197–200, 2009.

[12] M. Hioki and H. Kawasaki, "Estimation of Finger Joint Angles from sEMG Using a Neural Network Including Time Delay Factor and Recurrent Structure," *ISRN Rehabil.*, vol. 2012, pp. 1–13, 2012.

[13] J. Ngeo, T. Tamei, and T. Shibata, "Estimation of continuous multi-DOF finger joint kinematics from surface EMG using a multi-output Gaussian Process," in *2014 36th Annu*, 2014: Int. Conf. IEEE Eng. Med. Biol. Soc. EMBC, 2014, pp. 3537–3540.

[14] C. Chen, G. Chai, W. Guo, X. Sheng, D. Farina, and X. Zhu, "Prediction of finger kinematics from discharge timings of motor units: Implications for intuitive control of myoelectric prostheses," *J. Neural Eng*, vol. 16, p. 2, 2019.

[15] D. Blana, W. Murray, A. Ganguly, A. Krasoulis, K. Nazarpour, and E. Chadwick, "Model-based control of individual finger movements for prosthetic hand function," *Keele Univ*, pp. 1–9, 2019.

[16] S. Muceli and D. Farina, "Simultaneous and proportional estimation of hand kinematics from EMG during mirrored movements at multiple degrees-of-freedom," *IEEE Trans. Neural Syst. Rehabil. Eng*, vol. 20, no. 3, pp. 371–378, 2012.

[17] W. Li, P. Shi, and H. Yu, "Gesture Recognition Using Surface Electromyography and Deep Learning for Prostheses Hand: State-of-the-Art, Challenges, and Future," *Front Neurosci*, vol. 15, p. 259, Apr. 2021, doi: 10.3389/FNINS.2021.621885/BIBTEX.

[18] N. J. Jarque-Bou, J. L. Sancho-Bru, and M. Vergara, "A systematic review of EMG applications for the characterization of forearm and hand muscle activity during activities of daily living: Results, challenges, and open issues," *Sensors*, vol. 21, no. 9. MDPI AG, May 01, 2021. doi: 10.3390/s21093035.

[19] C. Boudreau, J. Corkum, I. Grant, and D. T. Tang, "A comparative study using electromyography to assess hand exercises for rehabilitation after ulnar nerve decompression," *Journal of Plastic, Reconstructive & Aesthetic Surgery*, vol. 75, no. 1, pp. 307–313, Jan. 2022, doi: 10.1016/J.BJPS.2021.08.042.

[20] A. A. Adewuyi, L. J. Hargrove, and T. A. Kuiken, "An Analysis of Intrinsic and Extrinsic Hand Muscle EMG for Improved Pattern Recognition Control," in *IEEE Trans*, vol. 24, no. 4: neural Syst. Rehabil. Eng. a Publ. IEEE Eng. Med. Biol. Soc, 2016, pp. 485–494.

[21] K. Fujimura, H. Kagaya, and H. Tanikawa, "Kinematic Analysis for Repetitive Peripheral Magnetic Stimulation of the Intrinsic Muscles of the Hand," *Applied Sciences (Switzerland)*, vol. 12, no. 18, Sep. 2022, doi: 10.3390/app12189015.

[22] M. Barsotti, S. Dupan, I. Vujaklija, S. Došen, A. Frisoli, and D. Farina, "Online Finger Control Using High-Density EMG and Minimal Training Data for Robotic Applications," *IEEE Robot Autom Lett*, vol. 4, no. 2, pp. 217–223, Apr. 2019, doi: 10.1109/LRA.2018.2885753.

[23] E. J. Weiss and M. Flanders, "Muscular and postural synergies of the human hand," *J. Neurophysiol.*, vol. 92, no. 1, pp. 523–535, 2004.

[24] S. Tateno, H. Liu, and J. Ou, "Development of sign language motion recognition system for hearing-impaired people using electromyography signal," *Sensors (Switzerland)*, vol. 20, no. 20, pp. 1–22, Oct. 2020, doi: 10.3390/s20205807.

[25] I. Carpinella, P. Mazzoleni, M. Rabuffetti, R. Thorsen, and M. Ferrarin, “Experimental protocol for the kinematic analysis of the hand: Definition and repeatability,” *Gait Posture*, vol. 23, no. 4, pp. 445–454, 2006.

[26] T. Bao, A. Zaidi, S. Xie, and Z. Zhang, “Surface-EMG based Wrist Kinematics Estimation using Convolutional Neural Network,” *p*, pp. 1–4, 2019.

[27] A. Sharma, P. Madhushri, V. Kushvaha, and A. Kumar, “Prediction of the Fracture Toughness of Silicafilled Epoxy Composites using K-Nearest Neighbor (KNN) Method,” *2020 International Conference on Computational Performance Evaluation, ComPE 2020*, pp. 194–198, Jul. 2020, doi: 10.1109/COMPE49325.2020.9200093.

[28] U. Phutane, M. Roller, A. Boebel, and S. Leyendecker, “Optimal control of grasping problem using postural synergies,” in *Advances in Transdisciplinary Engineering*, Aug. 2020, vol. 11, pp. 206–213. doi: 10.3233/ATDE200026.

[29] J. A. Raszewski, A. C. Black, and M. Varacallo, “Anatomy, Shoulder and Upper Limb, Hand Compartments,” *StatPearls*, Sep. 2022, Accessed: Dec. 09, 2022. [Online]. Available: https://www.ncbi.nlm.nih.gov/books/NBK532942/

[30] N. J. Jarque-Bou, M. Vergara, J. L. Sancho-Bru, V. Gracia-Ibáñez, and A. Roda-Sales, “A calibrated database of kinematics and EMG of the forearm and hand during activities of daily living,” *Sci Data*, vol. 6, no. 1, Dec. 2019, doi: 10.1038/s41597-019-0285-1.

[31] X. Hu, A. Song, J. Wang, H. Zeng, and W. Wei, “Finger Movement Recognition via High-Density Electromyography of Intrinsic and Extrinsic Hand Muscles,” *Sci Data*, vol. 9, no. 1, p. 373, 2022, doi: 10.1038/s41597-022-01484-2.

[32] B.-S. Lin, I.-J. Lee, P.-Y. Chiang, S.-Y. Huang, and C.-W. Peng, “A Modular Data Glove System for Finger and Hand Motion Capture Based on Inertial Sensors,” in *J*, vol. 39, no. 4: Med. Biol. Eng, 2019, pp. 532–540.